

Using of Automatic Slice-based Adjustment of Golem Voxel Phantom for Developing of Sudanese Voxel Phantom

Elhussien H.M. Sirelkhatim¹, A.M. Artoli², and Mohamed Osman³

¹Medical Physics Department,
Radiation & Isotopes Centre Khartoum, Khartoum, Sudan (RICK),
Khartoum, Sudan

²Department of Computer Science,
College of Computer and Information Sciences, King Saud University,
Riyadh 11543, KSA

³Department of Medical Physics,
Faculty of Science and Technology, Alneelain University,
Khartoum, Sudan

Copyright © 2016 ISSR Journals. This is an open access article distributed under the *Creative Commons Attribution License*, which permits unrestricted use, distribution, and reproduction in any medium, provided the original work is properly cited.

ABSTRACT: Developing of voxel phantoms has been an active field of research during the last decades and is receiving more attention nowadays. Reference phantoms for several ethnic groups have been developed recently as an extension to the ICRP reference phantoms that are based on Caucasian standard anatomical data,. This work reports an attempt to develop a tool for automatic slice-based adjustment of voxel phantoms. This tool achieves the adjustment process depending on anthropomorphic data extracted from anterior and lateral images for targeted body. The software was used to adjust Golem voxel model according to 23 Sudanese individuals. The weight, height, and age of these individuals vary from 52 to 113 Kg; from 166 to 188 cm and from 20 to 35 years, respectively. The maximum equivalent diameter, mean equivalent diameter, major axis length, minimum axis length, solidity and volume of brain, heart, kidneys, liver, lungs, spleen and bladder were calculated for all prepared models. For each organ, the mean value for each of these parameters was calculated and the deviation of each model from this value was evaluated. For the obtained data, we have calculated a global deviation of model (GDM) and selected the model with the smallest GDM to be the Sudanese voxel model. We have also compared volume, height and weight for 17 organs of the Sudanese voxel phantoms with ICRP phantom Golem + visible human and voxel man model.

KEYWORDS: voxel phantoms, nation specific voxel phantoms, Sudanese phantom, computational dosimetry, Slice-based adjustment.

1 INTRODUCTION

Developing of anthropomorphic computational models has been an active field of research during the last 50 years [1], [2]. The first generation is the stylized or mathematical phantoms which started in 1960's. The first mathematical model was developed by Fisher and Synder using simple geometrical shapes [3]. This model is homogeneous and hermaphrodite and contains three regions: head and neck, trunk including arms, and legs. Synder et al. improved this model to be heterogeneous with different densities given for lung, bones and soft tissues [4]. The improved model is known as MIRD after the Medical Internal Radiation Doses Committee. Fisher and Synder [3] scaled down this model to cover pediatrics. In 1967 three designed phantoms for new born, ten and fifteen years old were developed separately [5], [9]. In 1980 Cristy developed a complete family of mathematical phantoms [10], including adult, new born, one, five, ten and fifteen years old

phantoms. An improved version of these phantoms was developed by Cristy and Eckerman [11]. This improved version was known as ORNL family after Oak Ridge National Laboratory.

In 1982, Kramer et al. used MIRD as base to develop ADAM and EVA as the first gender specific mathematical models [12]. In 1995 Stabin et al. developed three mathematical models for a pregnant female in the first, second and third trimester of pregnancy [13].

Voxel model is the second generation of anthropomorphic phantoms which appeared as a result of the evolution on tomographic medical imaging and computer technology. The first voxel model was developed in 1984 by Gibbs [14-16]. Then in 1986 a research group from GSF developed two pediatric phantoms, later extended to cover a family of voxel phantoms. Two of these phantoms are REX and REGINA which are adapted according to ICRP reference man and woman [17] and adopted as standard voxel models of ICRP [18]. In 1994, Zubal et al. developed a model called VOXELMAN [19] and then Kramer et al. developed a modified version of this model called MAX [20]. MAX has been adjusted according to ICRP reference man. Kramer et al. also developed FAX [21] a female voxel phantom adjusted according to ICRP-89 reference woman. These two models have been modified to satisfy ICRP-103 recommendations [22]. The results are MAX06 and Fax06 [23].

Beside the two pediatric phantoms mentioned above, a number of other pediatric voxel models have been developed. In 1999 Caon et al. developed the ADELAIDE model of a fourteen years old girl [24]. In 2002 Nipper et al. from University of Florida (UF) developed UF new born and UF2 for two-month old models [25] Then Lee et al. developed the series of UF Head-Torso pediatric phantoms which cover ages from nine months to fourteen years [26] and second series of pediatric whole-body phantoms [27].

In 1995 Dimbylow used MRI images to develop NORMAN and NAOMI male and female phantoms. Later he used NAOMI to develop a series of pregnant women models [28]. Other pregnant models were developed by Shi et al [29] and Cech [30]. Beside CT and MRI images, a number of models have been developed using color cross sectional images of cadavers. The first of these models was developed by Xu et al in 2000. To cover anatomical variation between deferent races, research groups from Japan, Korea and China developed voxel phantoms having the standard body characteristics of their ethnic group. Saito et al from Japan developed OTOKO, JM and JM2, three voxel models of adult men in addition [31], [34] to ONAGO and JF [30], [32], two voxel models of adult females. Nagaoka et al also from Japan used sets of MRI to develop TARO and HANAKO, two adult male and female voxel models [35] developed for studies of non-ionizing radiations. Beside these two models, Nagaoka et al developed three pediatric voxel models represent three, five and seven years old Japanese children [36]. The pediatric phantoms were modeled using Free Form Deformation (FFD) algorithm [37]. Nagaoka et al also used FFD algorithm to develop voxel models in different postures [38], [39]. In addition to these Japanese voxel models five voxel models from Korea [40], [44] and three voxel models from China [45], [50] had been developed. Recently other models represent Syrian [51] and Iranian [52], [53] ethnic groups have been developed

In this work we adjust a voxel phantom according to anthropomorphic data of 23 Sudanese individuals. For the adjustment process, we developed a dedicated software for slice-based automatic processing. This strategy was used as a relatively simple method to create a Sudanese voxel phantom starting from an existing voxel model.

2 METHOD

2.1 AUTOMATIC SLICE-BASED ADJUSTMENT OF VOXEL PHANTOMS

Many reports in the literature consider modeling of 3D objects according to data extracted from 2D images [54], [56]. We found a good starting point on the work of Charlie et al [57], which consider adaptation of human surface model according to two orthogonal images of a target body. They adapt the position of specific points on the surface of the source model according to two orthogonal images of the target body. However, in their case and unlike voxel phantoms the source model is a surface model without internal anatomy. To deal with voxel phantoms we adopt the following scenario. Initially we partition the model into seven parts. Then we adjust the position of internal organs with respect to the Z-direction. After this, we append, re-slice and adapt the segments in the X and Y directions.

We developed a Matlab code with general flow illustrated in Fig. 1. The code considers Z axis to points from head to foot, X axis to points from right to left and Y axis to points from front to back.

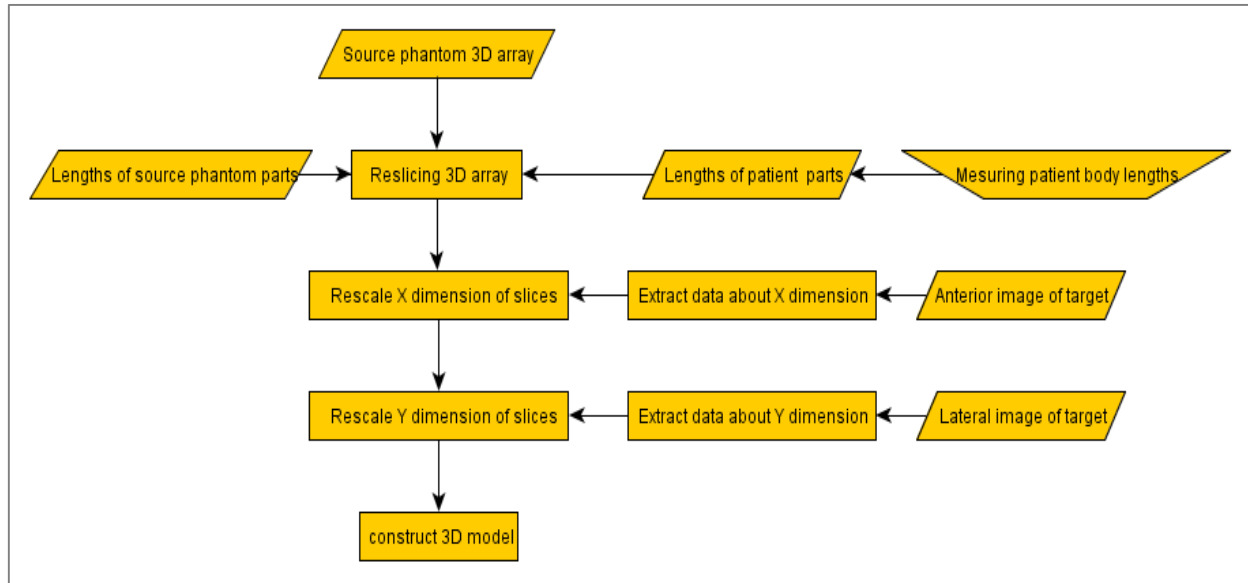


Fig. 1. Scenario of the algorithm developed for automatic slice-based adjustment of source voxel phantom.

At first, the user has to import the source phantom model. The code assumes this model to be without arms, legs or ears and has seven segments in Z direction the first of these segments goes from top of head down to the nasion. The second to the end of the nose, the third to the bottom of the chin, the fourth to the level of the seventh cervical vertebra, the fifth to the level of the xiphoid process, the sixth to the level of the iliac crest and the seventh segment goes down to the end of the model. To start the adjustment process, the user has to insert the length of the seven segments for the source phantom and the targeted body in addition to the number of slices of the source phantom to be prepared. The user has also to pick anterior and lateral silhouette images of the target body and give their magnification factors. These two images must have the same heights and are assumed to be without ears, arms and legs. The reason of removing these parts is the discontinuity of their borders which will disturb the code. At the beginning, the code starts by preparing the slices of the source phantom in 3D array. Then, in order to adapt in Z direction, it prepares a number of slices from each segment according to the following equation:

$$(NS)_i = \text{round} [(TL)_i / NST] \quad (1)$$

Where NS , TL , NST , and i represent number of slices to be prepared, target length of segment, new slice thickness, and segment number respectively. To adapt the source model in X direction, the code scans the anterior image from top to bottom with steps equal NST . In each step, it calculates the length between the borders of the body at the position of that step on the image. Then the code normalizes these lengths according to the largest length of them ($-ML-$) and stores the normalized lengths the (NL) . After that the code starts scanning the prepared slices of the source model one by one from top to bottom. For each slice, it crops the area of the slice which contains source model body and stores its length in X direction another. The length of the cropped image which faces (ML) will be considered as the normal source model length (NSL) . Then, the new length in X direction of the cropped image number i which represented with NCL_i can be calculated by using the following equation:

$$NCL_i = NSL * NL_i \quad (2)$$

After changing the lengths of the cropped images in X direction according to the calculated values, the code pastes these images again in their original slices. By this way the slices would keep their number of pixels but the dimension of these pixels would be modified. To calculate the new dimension of pixels in X direction NPD , the code uses the following equation:

$$NPD = (ML * APD) / NSL \quad (3)$$

Where APD represents the pixel dimensions of the anterior image. This step completes adapting of the model in X direction. To adapt in Y direction the code repeats these steps using the lateral image of the target body.

2.2 PREPARATION OF THE SOURCE VOXEL MODEL

In this study we used Golem voxel phantom (58) as source model. This model was developed from CT images of a 38 years old patient with height of 176 cm and weight of 68.9 kg. The model consists of 220 slices with 256x256 pixels. The voxel dimensions are 0.208x 0.208 x 0.805cm³. At first data of the phantom was prepared into slices. The result is shown in Fig. 2. Then ears, arms and legs were removed, after that the model was divided into the mentioned seven segments.

The reference planes used for segmentation are shown in Fig. 3. The lengths of these segments in addition to Golem slices are passed to the code.

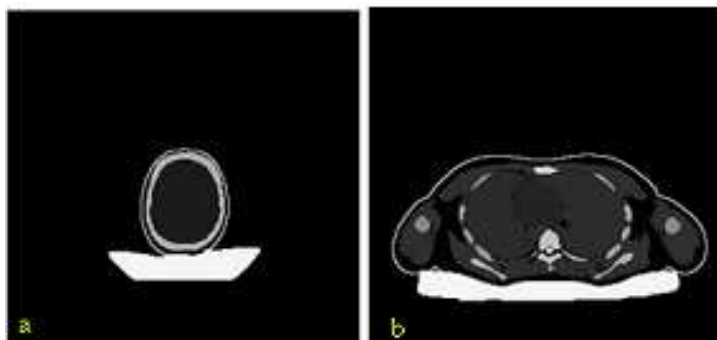


Fig. 2. Sample of Golem slices, from head (a) and chest (b).

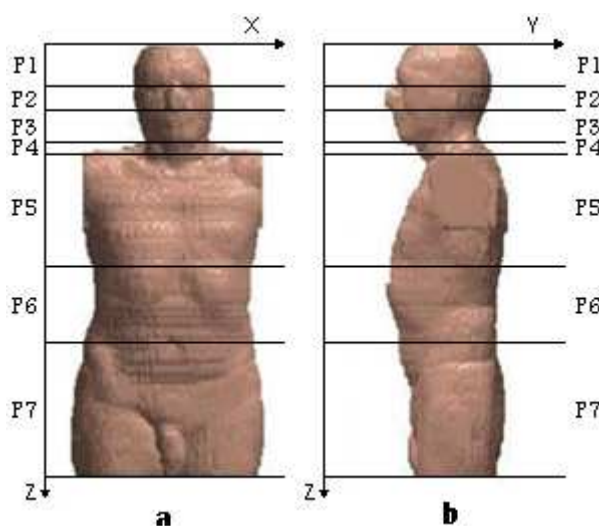


Fig. 3. 3D Rendering of Golem model after removing ears, hands and legs. (a) Anterior view. (b) Lateral view. Shown are the reference planes used for segmentation

2.3 DATA COLLECTING AND PROCESSING

Anterior and lateral images for 23 Sudanese volunteers were acquired. The weight, height and age of these individuals vary from 52 to 113; from 166 to 188 and from 20 to 35 respectively. Each of the individuals was asked to wear as tight as possible clothes. The camera was held vertically without tilting. Distance and magnification of imaging are adapted to satisfy the height of each individual. For each individual, the anterior image was acquired at first; then the lateral image was acquired with the same parameters. The magnification factor of each image was calculated by comparing the actual length of the second segment with its length in the image. Then, silhouette versions of these images are prepared after removing arms, ears and legs and treating defects resulted due to wear less or very tightly clothes. Samples of these images are shown in Figure 4. From these images, the lengths of body segments are measured in pixels for each individual. The source voxel model was adjusted according to these data to generate 23 voxel models. Then, the maximum equivalent diameter, mean equivalent diameter, major axis length, minimum axis length, solidity and volume of brain, heart, kidneys, liver, lungs, spleen and bladder were calculated for each model.

For each organ, the mean values of these parameters were calculated and used to evaluate what was then called Global Deviation of Model (GDM) by using the following equation:

$$GDM_i = \sum_j \sum_k D_{i,j,k} \quad (4)$$

Where $D_{i,j,k}$ is the deviation of the model i for the parameter k of the organ j . From the statistical point of view the model with the smallest GDM is the best representation of all models and therefore it will be selected as the Sudanese voxel phantom.

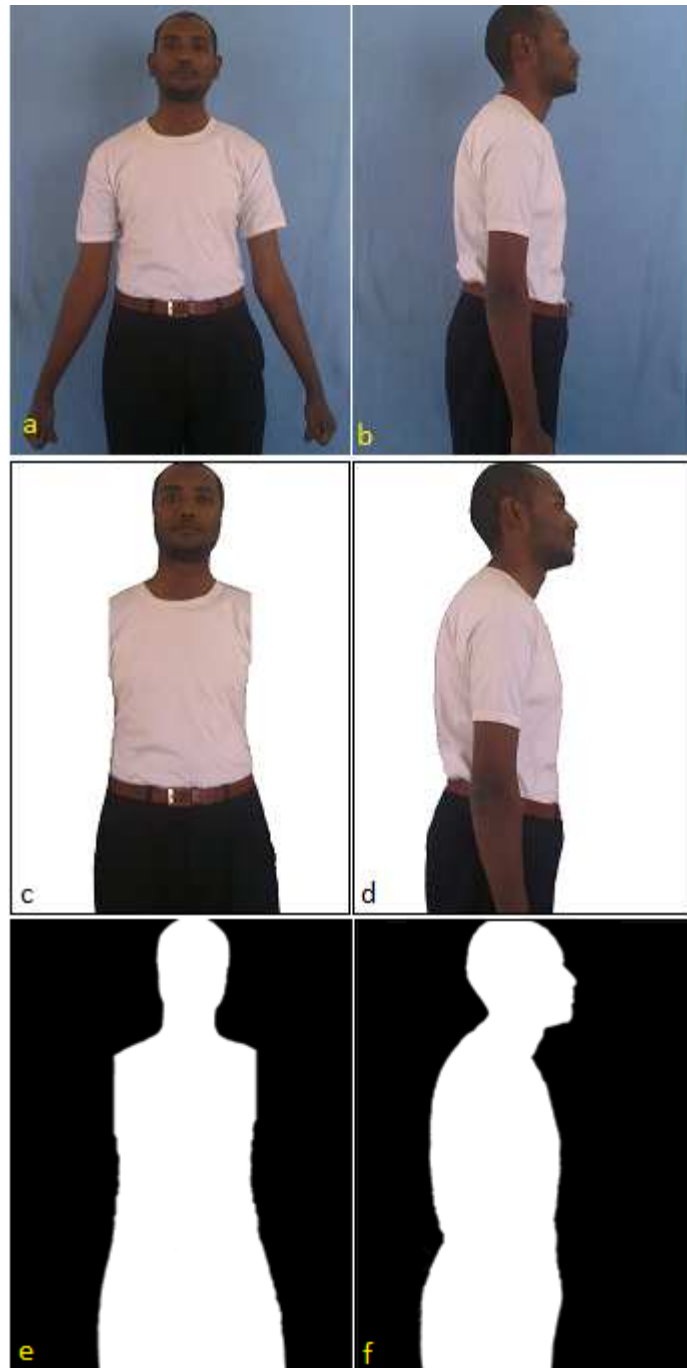


Fig. 4. Images for one of the 23 Sudanese individuals who participated in the study to develop the Sudanese voxel phantom. Shown are the different stages of preparation. Images (a) and (b) are the original anterior and lateral images respectively, images (c) and (d) are the same images after removing ears, arms and background while (e) and (f) are the final silhouette images.

3 RESULTS

The maximum equivalent diameter, mean equivalent diameter, major axis length, minimum axis length, and volume for of the nine organs mentioned above were calculated.

As Sample, results of these parameters for liver are shown in Fig. (5-9). The normality of distribution was examined against Gaussian distribution .the p value of the test was found to be greater than 0.05 for all parameters of all organs as example for liver the values are: 0.126, 0.242, 0.158, 0.109 and 0.142 for the mentioned parameters respectively. There for Gaussian distribution is considered to be acceptable approximation for distribution of these parameters. This means that the parameters of the adjusted models and there organs have the same statistical distribution as those of actual population.

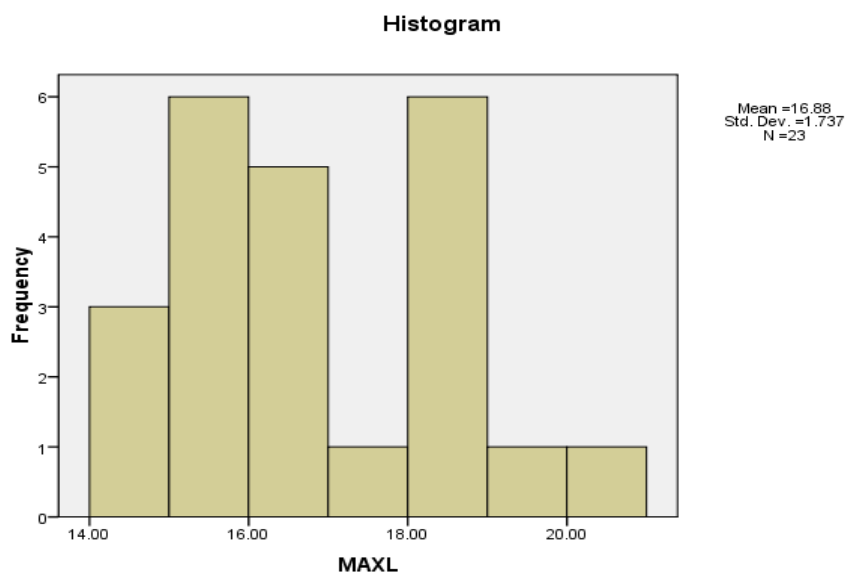


Fig. 5. Lengths of maximum and mean equivalent diameters in addition to major and minor axis of brain for 23 Sudanese individuals participated in the study to develop Sudanese voxel phantom.

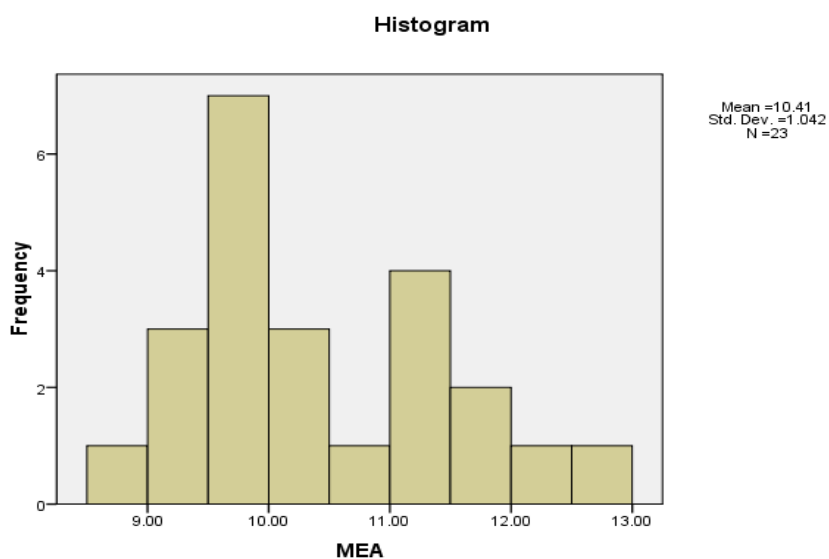


Fig. 6. Lengths of maximum and mean equivalent diameters in addition to major and minor axis of spleen for 23 Sudanese individuals participated in the study to develop Sudanese voxel phantom

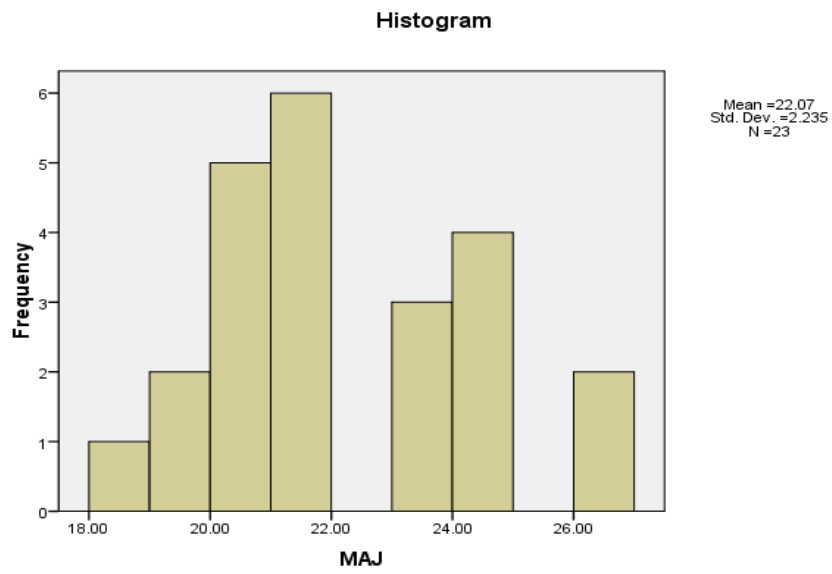


Fig. 7. The solidity of right kidney for the 23 Sudanese individuals participated in the study to develop Sudanese voxel phantom

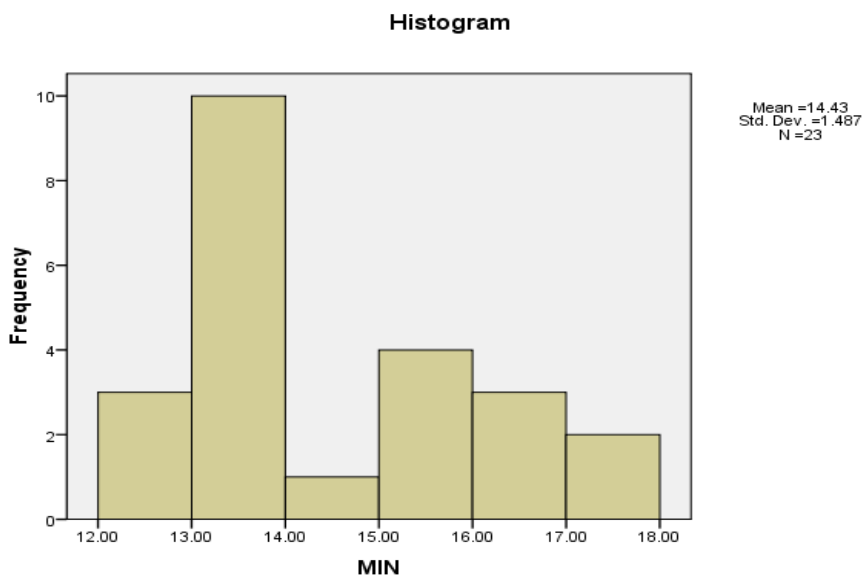


Fig. 8. The solidity of left lung for the 23 Sudanese individuals participated in the study to develop Sudanese voxel phantom

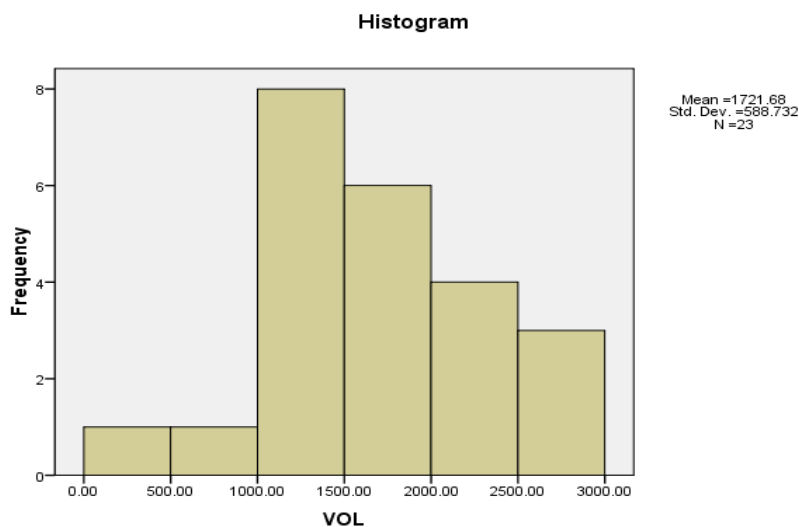


Fig. 9. The volume of heart for the 23 Sudanese individuals participated in the study to develop Sudanese voxel phantom

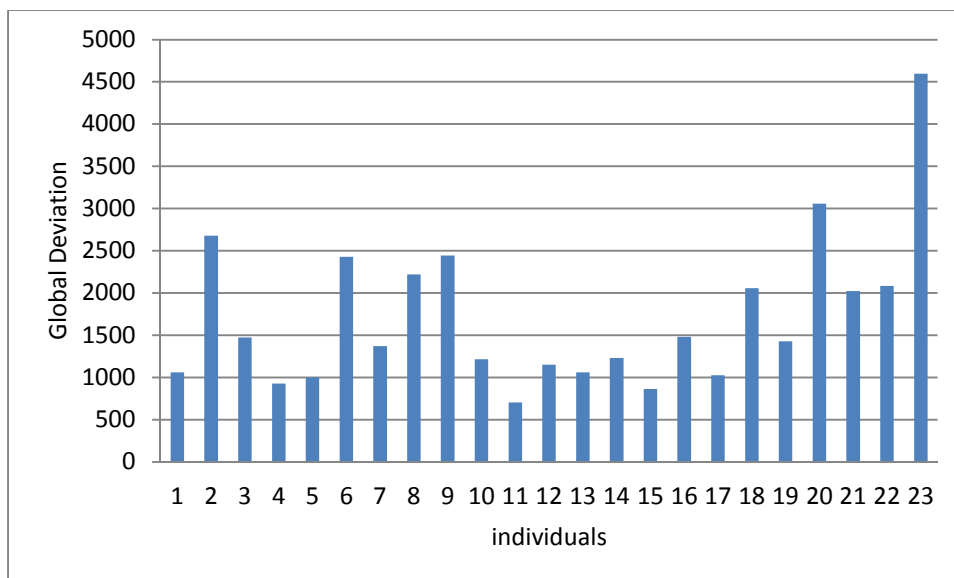


Fig. 10. The volume of liver for the 23 Sudanese individuals participated in the study to develop Sudanese voxel phantom

The maximum, minimum and average of these parameters were evaluated for the nine organs of the 23 models. Then, equation (4) is used to calculate the *GDM* for each individual. The results are explored in Fig. 11. It can be seen that the individual number 11 has the minimum *GDM*. Therefore, it was selected as the Sudanese voxel phantom.

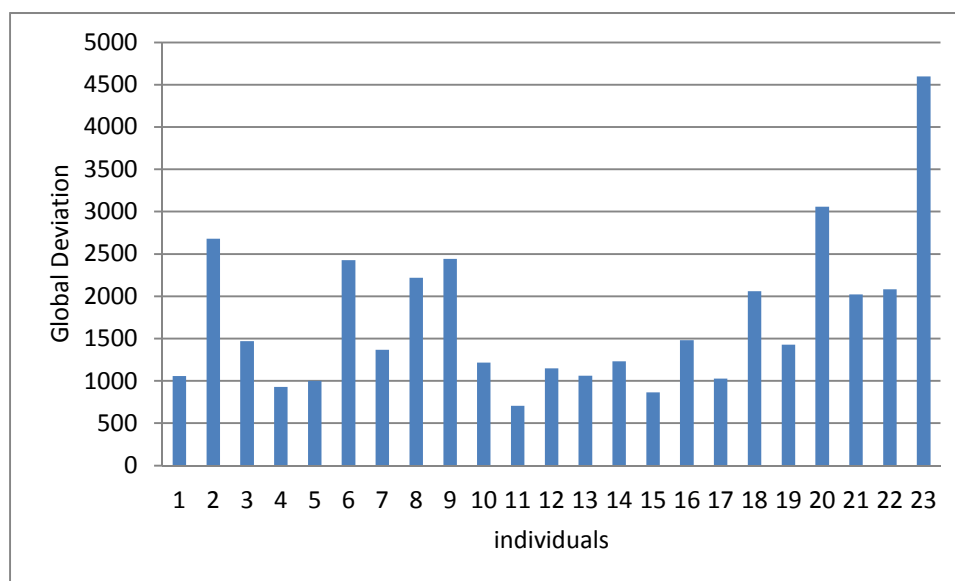


Fig. 11. The Global Deviation for the 23 individuals participated in the study to develop Sudanese voxel phantom

4 DISCUSSIONS

Table 1 contains the volume of selected organs of the Sudanese voxel phantom in addition to the weight and height in comparison with those of ICRP reference man, Golem, Visible Human and Voxel man models.

Table 1. Comparison of organ masses -in gram- and total body height – in centimetre - of Sudanese voxel phantom, ICRP reference man, Golem, Visible Human and voxel man models

Organ	Sudanese Phantom	ICRP reference man	Golem	Visible Human	VOXELMAN
Adrenals	17.5	14	22.8	8.3	4.2
Bladder	61.1	45	68.4	41.4	212
Brain	1399	1400	1218	1574	1230
Eye lenses	0.9	0.4	0.94	0.54	1.55
Gall bladder	8.3	10	8.29	12	22.1
Heart	699.8	330	716	399	629
Kidneys	310.8	310	316	335	512
Liver	1441	1800	1592	1938	1967
Lungs	699.4	1000	747	911	1038
Esophagus	23.9	40	30.1	69.1	43.1
Pancreas	72	100	71.9	82.9	53.2
Prostate	56.8	16	54.7	18.9	29.4
Spleen	153.4	180	174	244	374
Stomach	126.2	150	233	173	345
Testes	23.1	35	21.1	21	116
Thyroid	19.4	20	25.8	27.6	7.1
Trachea	10.4	10	13.7	–	57.8
Total body (Kg)	65	70	68.93	103.176	70.215
Total body height (cm)	174	176	176	180	178

All the phantoms are compared to ICRP reference phantom. We can see that for adrenals, brain, gall bladder, kidneys, testes, thyroid and trachea the relative variation of Sudanese phantom has the minimum variation compared with other phantoms, while for bladder, spleen, total weight and height the values for the Sudanese phantom is near to the minimum values of variation. For eyes lenses, esophagus and pancreas the values for Sudanese phantom are near to the medium. For the heart the variation of the Sudanese phantom is near to the maximum value. In case of liver, lungs and prostate, the

variation has the maximum value. Here we can note that, these values are near to those of Golem. Therefore, we can conclude that, these large variations are due to the large relative variation of the used source model in comparison to ICRP phantom.

5 CONCLUSIONS

In this study, we have developed a Sudanese voxel phantom. To our knowledge, this is the first African nation's specific voxel phantom. This opens the door for other studies to calculate different dosimetric conversion factors more accurately. The relatively simple approach suggested in this work can serve in improving some of new emerging concepts in radiation protection such as developing of virtual population, developing of statistical voxel phantoms [59] and developing a library of patient dependent voxel phantoms for patient-phantom matching.

ACKNOWLEDGEMENTS

We thank GSF institute for the permission to use Golem voxel phantom and Dr Maria Zankel for her appreciated scientific advisements

REFERENCES

- [1] Loevinger R. Distributed radionuclide sources. In AttixFH, Tochilin E, eds. Radiation Dosimetry Volume III, 2nd edn. New York: Academic Press, 1969.
- [2] Ulam SM. On the Monte Carlo method. in Symposium on Large-Scale Digital Calculating Machines, Cambridge, MA 1949; 207-1 2
- [3] Fisher H, Snyder W. Variation of dose delivered by ¹³⁷Cs as a function of body size from infancy to adulthood. ORNL-4007. Rep. TN 221–28. Oak Ridge, TN: Oak Ridge Natl. Lab. 1966.
- [4] Snyder WS, et al. Estimates of absorbed fractions for monoenergetic photon sources uniformly distributed in various organs of a heterogeneous phantom. J Nucl Med 1969; 10 (Suppl. 3): 7.
- [5] Snyder WS, Ford MR, Warner G. Estimates of Specific Absorbed Fractions for Photon Sources Uniformly Distributed in Various Organs of a Heterogeneous Phantom. New York.
- [6] Hwang JML et al. Mathematical description of a one- and five-year-old child for use in dosimetry calculations. Oak Ridge, TN: Oak Ridge National Laboratory; 1976. ORNL/TM-5293.
- [7] Hwang JML, Shoup RL, Poston JW. Mathematical description of a newborn human for use in dosimetry calculations. Oak Ridge, TN: Oak Ridge National Laboratory; 1976. ORNL/TM-5453.
- [8] RM Jones, et al. The development and use of a fifteen-year-old equivalent mathematical phantom for internal dose calculations, Oak Ridge, TN: Oak Ridge National Laboratory; 1976. ORNL/TM-5278.
- [9] Deus SF, Poston JW. The development of a mathematical phantom representing a 10-year-old for use in internal dose calculations. Proceedings of the Symposium on Radiopharmaceutical Dosimetry; Oak Ridge, TN: Oak Ridge National Laboratory; 1976. HEW Publication (FDA) 76-8044.
- [10] Cristy M. Mathematical phantoms representing children of various ages for use in estimates of internal dose. Oak Ridge, TN: Oak Ridge National Laboratory; 1980. ORNL/NUREG/TM-367.
- [11] Cristy M, Eckerman KF. Specific absorbed fractions of energy at various ages from internal photon sources. Oak Ridge, TN: Oak Ridge National Laboratory; 1987. ORNL/TM-8381.
- [12] R. Kramer et al. The calculation of dose from external photon exposures using reference human phantoms and Monte Carlo methods: Part I. The male (ADAM) and female (EVA) adult mathematical phantoms. Neuherberg-Muenchen: GSF-National Research Center for Environment and Health; 1982. GSF-Report S-885.
- [13] Stabin MG, et al. Mathematical models and specific absorbed fractions of photon energy in the nonpregnant adult female and at the end of each trimester of pregnancy. Oak Ridge, TN: Oak Ridge National Laboratory; 1995. ORNL/TM-12907.
- [14] Gibbs S and Pujol J. A Monte Carlo method for patient dosimetry from diagnostic x-ray. Dentomaxillofac Radiol 1982; 11(25).
- [15] Gibbs S et al. Radiation doses to sensitive organs from intraoral dental radiography Dentomaxillofac Radiol 1987; 16: 67–77.
- [16] Gibbs SJ, Pujol A, Chen TS, et al. Patient risk from interproximal radiography, Oral Surg Oral Med Oral Pathol Oral Radiol Endod 1984; 58(3):347-54.

- [17] ICRP. Basic Anatomical and Physiological Data for Use in Radiological Protection: Reference Values, International Commission on Radiological Protection (ICRP) Publication 89, Pergamon Press, Oxford, 2002.
- [18] International Commission of Radiological Protection. ICRP Publication 110. Adult Reference Computational Phantoms. Amsterdam: Elsevier; 2009.
- [19] Zubal IG, Harrell CR, Smith EO, et al. Computerized three-dimensional segmented human anatomy, *Med Phys* 1994; 21: 299-302.
- [20] Kramer R, Khoury HJ, Vieira JW, et al. All about MAX: A male adult voxel phantom for Monte Carlo calculations in radiation protection dosimetry. *Phys Med Biol* 2003; 48(10): 1239-1262.
- [21] Kramer R, Khoury HJ, Vieira JW, et al. All about FAX: A female adult voxel phantom for Monte Carlo calculation in radiation protection dosimetry. *Phys Med Biol* 2004; 49(23): 5203-5216.
- [22] ICRP. The 2007 Recommendations of the International Commission on Radiological Protection. ICRP Publication 103, *Ann. ICRP*, 37, 1, 2007.
- [23] Kramer R, Khoury HJ, Vieira JW. MAX06 and FAX06: Update of two adult human phantoms for radiation protection dosimetry. *Phys Med Biol* 2006; 51(14): 3331-3346.
- [24] Caon M, Bibbo G and Pattison J. An EGS4-ready tomographic computational model of a 14-year-old female torso for calculating organ doses from CT examinations, *Phys Med Biol* 1999; 44(9) 2213-2225.
- [25] JC Nipper, JL Williams and WE Bolch. Creation of two tomographic voxel models of pediatric patients in the first year of life. *Phys Med Biol* 2002; 47: 3143.
- [26] Lee C, et al. The UF series of tomographic computational phantoms of pediatric patients, *Med Phys* 2005; 32(6): 3537-3548.
- [27] Lee C, et al. Whole-body voxel phantoms of pediatric patients—UF Series B. *Phys Med Biol* 2006; 51:4649.
- [28] Dimbylow PJ. Development of pregnant female, hybrid voxel-mathematical models and their application to the dosimetry of applied magnetic and electric fields at 50 Hz, *Phys Med Biol* 2006; 51: 2383–2394.
- [29] Shi C Xu XG. Development of a 30-week-pregnant female tomographic model from computed tomography (CT) images for Monte Carlo organ dose calculations. *Med Phys* 2004; 31: 2491.
- [30] Cech R, Leitgeb N, Pediaditis M. Fetal exposure to low frequency electric and magnetic fields. *Phys Med Biol* 2007;52(4):879.
- [31] Saito K, et al. Construction of a computed tomographic phantom for a Japanese male adult and dose calculation system. *Radiat. Environ. Biophys* 2001; 40: 69.
- [32] Sato K, et al. Japanese adult male voxel phantom constructed on the basis of CT images. *Radiat Prot Dosim* 2007; 123: 337.
- [33] Sato K, et al. Development of a voxel phantom of Japanese adult male in upright posture, *Radiat Prot Dosim* 2007; 127, p.205.
- [34] Saito K, et al. Construction of a voxel phantom based on CT data for a Japanese female adult and its use for calculation of organ doses from external electrons. *Japanese Journal of Health and Physics* 2008; 43: 122.
- [35] Lee C, Nagaoka T and Lee JK. Implementation of Japanese male and female tomographic phantoms to multi-particle Monte Carlo code for ionizing radiation dosimetry. *J Nucl Sci Technol* 2006; 43: 937.
- [36] Nagaoka T, Kunieda E and Watanabe S. Proportion-corrected scaled voxel models for Japanese children and their application to the numerical dosimetry of specific absorption rate for frequencies from 30 MHz to 3 GHz. *Phys Med Biol* 2008; 53: 6695.
- [37] Sederberg TW, Parry SR. Free-form deformation of solid geometric models. In SIGGRAPH '86: Proceedings of the 13th annual conference on Computer graphics and interactive techniques. New York: ACM Press; 1986. p151–160.
- [38] Nagaoka T, Watanabe S. Development and application of human voxel models in Japan. *International Zurich Symposium on Electromagnetic Compatibility*, Suntec City: Singapore 2006;17:59.
- [39] Nagaoka T and Watanabe S. Postured voxel-based human models for electromagnetic dosimetry. *Phys Med Biol* 2008; 53: 7047.
- [40] Lee C, Lee J and Lee C. Korean adult male voxel model KORMAN segmented from magnetic resonance images. *Med Phys* 2004; 31: 1017.
- [41] Lee C, Lee J. Reference Korean human models: Past, present, and future. In *The Monte Carlo Method: Versatility Unbounded in a Dynamic Computing World*, Chattanooga, TN, 2005 April 17–21.
- [42] Lee C, et al. Development of the two Korean adult tomographic computational phantoms for organ dosimetry. *Med Phys* 2006; 33: 380.
- [43] Choi SH et al. Construction of a highdefinition 'Reference Korean' voxel phantom for organ and tissue radiation dose calculation. In *World Congress on Medical Physics and Biomedical Engineering*, Seoul, Korea, 2006.
- [44] Kim CH, et al. HDRK-Man. A whole-body voxel model based on high-resolution color slice images of a Korean adult male cadaver. *Phys Med Biol* 2008; 53: 4093

- [45] Zhang B, Ma J, Liu L, Cheng J CNMAN. A Chinese adult male voxel phantom constructed from color photographs of a visible anatomical data set. *Radiat Prot Dosim* 2007;124(2): 130-136.
- [46] Zhang G, et al. Organ dose calculations by Monte Carlo modeling of the updated VCH adult male phantom against idealized external proton exposure. *Phys Med Biol* 2008; 53: 3697.
- [47] Zhang G, et al. The development and application of the visible Chinese human model for Monte Carlo dose calculations. *Health Phys* 2008; 94: 118.
- [48] Zhang G, Liu Q and Luo QM. Monte Carlo simulations for external neutron dosimetry based on the visible Chinese human phantom. *Phys Med Biol* 2008;52: 7367.
- [49] Li, J.L. et al. Organ dose conversion coefficients for external photon irradiation using the Chinese Voxel Phantom (CVP), *Radiat Prot Dosim* 2009; 135(1): 33-42.
- [50] Zeng Z, et al. Dose assessment for space radiation using a proton differential dose spectrum. *J Tsinghua Univ (Sci Technol)* 2007; 46: 374.
- [51] Bashira Taleb, Ahmed Khadour, Abadalkader. Reconstruction of head-to-knee voxel model for Syrian adult male of average height and weight, *Egyptian Journal of Radiology and Nuclear Medicine* 2015; 3(2).
- [52] Akhlaghi P1, Hakimabad HM2, Motavalli LR1. Evaluation of dose conversion coefficients for an eight-year-old Iranian male phantom undergoing computed tomography, *Radiation and Environmental Biophysics*, 2015; Volume 54, Issue (4), pp 465-474.
- [53] Parisa Akhlaghi, Hashem Miri Hakimabad, Laleh Rafat Motavalli. Dose estimation for Iranian 11- year-old pediatric phantoms undergoing computed tomography examinations, *Journal of Radiation Research*, 2015; 56(4): 646-655.
- [54] G.A Bilodeau, R Bergevin. Generic Modeling of 3D Objects from single 2D images, *International Conference on Pattern Recognition (ICPR'00)*2000; 1,1770-1773.
- [55] Jalda Dworzak, Hans Lamecker, Jens von Berg et al. 3D Reconstruction of the Human Rib Cage from 2D Projection Images Using a Statistical Shape Model. *Int. J. Computer Assisted Radiology and Surgery* 2010;5(2): 111-124.
- [56] Tal Hassner and Ronen Basri, Example Based 3D Reconstruction from Single 2D Images, *Proceedings of the 2006 Conference on Computer Vision and Pattern Recognition Workshop 2006 IEEE; (CVPRW'06)*: 0-7695-2646-2/06.
- [57] Charlie C. L. Wang, Yu Wang Terry et al. Virtual human modeling from photographs for garment industry. *Computer-Aided Design*2003;(35):577-589.
- [58] Maria Zankl, Alfred Wittmann, The adult male voxel model "Golem" segmented from whole-body CT patient data. *Radiat Environ Biophys* 2001; 40:153-162.
- [59] George X, Tianyu L. Quantifying uncertainty in radiation protection dosimetry using statistical phantoms. Paper presented at: The third international workshop on computational phantoms for radiation protection, imaging and radiotherapy; 2011 Aug 8-9, Tsinghua University, Beijing, China.